COMPARISON OF MEASURED AND SIMULATED π/4-DQPSK ADJACENT CHANNEL POWER USING A FUNCTIONAL HIGH POWER AMPLIFIER MODEL

Mauri Honkanen[1*], Ossi Pöllänen[2], Juha Tanskanen[2], Esko Järvinen[2] and Sven-Gustav Häggman[3]

[1] Nokia Research Center, P.O. Box 100, FIN-33721 Tampere, Finland
[2] Nokia Research Center, P.O. Box 45, FIN-00211 Helsinki, Finland
[3] Helsinki University of Technology, Institute of Radio Communications, Communications Laboratory, P.O. Box 3000, FIN-02015 HUT, Finland

Abstract — A novel functional nonlinear high power amplifier model for radio communication system simulations is used to study spectrum regeneration of a nonlinearly amplified π/4-DQPSK signal. Simulated adjacent channel power has been compared to measured results, and a very good resemblance is found. This together with a satisfactory intermodulation behaviour in a two-tone test simulation verifies that the proposed model is applicable to accurate adjacent channel power prediction in radio system simulations.

I. INTRODUCTION

The target of efficient utilisation of scarce radio spectrum has signified a strong interest in linear modulation schemes which is indicated, for example, by the recent specification work on third generation mobile communication systems in Europe [1]. However, a fluctuating signal envelope is an inherent feature of linear modulation methods resulting in spectrum regeneration when a nonlinear high power amplifier (HPA) is used to amplify the signal. Spectral skirts of the signal act as interference to the adjacent channels, and some co-channel interference is also generated due to the signal distortion. Thus, these phenomena have a direct impact on the system capacity and performance. Still, a certain amount of HPA nonlinearity has to be accepted in order to guarantee satisfactory amplifier efficiency and to extend mobile phone usage time. Therefore an accurate and verified simulation model for an HPA is required to reliably study effects of nonlinearity on the system level, and to give an insight to the problem of finding a proper trade-off between HPA efficiency and system capacity.

A number of studies on spectrum regeneration have been presented on a general level, for instance, in [2-4]. In contrast to them, we will concentrate to evaluate the capabilities of a functional Class AB bipolar HPA model introduced in [5]. The model was designated for radio communication system simulations, and it was found to have an excellent two-tone test resemblance to a real mobile phone HPA. Because of the significant differences in amplitude and frequency distributions between a band-limited digitally modulated signal and a two-tone signal, comparisons between modelled and measured spectral regrowth of a modulated signal are required to further prove the validity of the model. The performance of the model by means of π/4-DQPSK spectrum regeneration is scrutinised here.

II. HPA MODEL DESCRIPTION

The nonlinear distortion caused by an HPA is here divided into separate behavioural amplitude and phase distortion models to be used with complex lowpass equivalent signals. Amplitude distortion is here regarded as the dominating counterpart in the nonlinearity as proposed in [5], even though some phase distortion is also generated by a real high power amplifier. Hence, accurate amplitude characteristics modelling is emphasised. The model represents bipolar amplifiers, since the same functional relationship is not capable of describing large-signal characteristics of both bipolar and FET amplifiers adequately because of the physical differences between these transistor types.

A. Amplitude Distortion Model

The functional HPA amplitude distortion model introduced in [5] has a substantiated semi-physical basis, since the nonlinear effect of the base-emitter junction of a Class AB bipolar HPA is taken into account in the form of an exponential envelope transfer characteristic in the low power region. As the input power grows the exponential behaviour turns into a linear one because of the feedback in the amplifier configuration. Linearity of an amplifier is strongly influenced by the biasing of the device. An inclusion of a biasing capability leads to an HPA input-output relationship defined by exponential and linear parts:

[*] The work was performed while the author was with Helsinki University of Technology, Institute of Radio Communications, Communications Laboratory.

$$V'_{out}(V_{in}) = e^{k\cdot(V_{in}+V_b)} - 1 - V_{out,zero} \\ = e^{k\cdot V_b}\left(e^{k\cdot V_{in}} - 1\right), \qquad V_{in}+V_b \le V_{in,tr} \quad (1)$$

$$V'_{out}(V_{in}) = v\cdot(V_{in}+V_b) + b - V_{out,zero} \\ = v\cdot(V_{in}+V_b) + b - e^{k\cdot V_b} + 1, \qquad V_{in}+V_b > V_{in,tr} \quad (2)$$

where the positive half cycle of a Class AB push-pull configuration HPA ($V_{in} \ge 0$) is assumed to take place. V_{in} is the instantaneous amplitude value of input signal envelope, v is the derivative of the linear part of the amplitude characteristic curve, k is the parameter which determines how steep the exponential curve is ($k \ge 0$) and V_b is the bias parameter adjusting the zero input amplitude location on the amplification curve as illustrated in Fig. 1. The corresponding output zero amplitude shift is given by

$$V_{out,zero} = e^{k\cdot V_b} - 1. \quad (3)$$

The transition from the exponential part to the linear one is continuous and occurs at the point

$$V_{in,tr} = \frac{1}{k}\ln\frac{v}{k} \quad (4)$$

and the value for b is given by

$$b = e^{k\cdot V_{in,tr}} - 1 - v\cdot V_{in,tr}. \quad (5)$$

Thus, whether the biased input amplitude value V_{in} + V_b is smaller or larger than $V_{in,tr}$, either (1) or (2) is employed, correspondingly. However, at a certain input power level the output starts to saturate due to the finite power supply. Rapp's saturation function [6] is utilised to produce a smooth transition from the linear region to the saturated one.

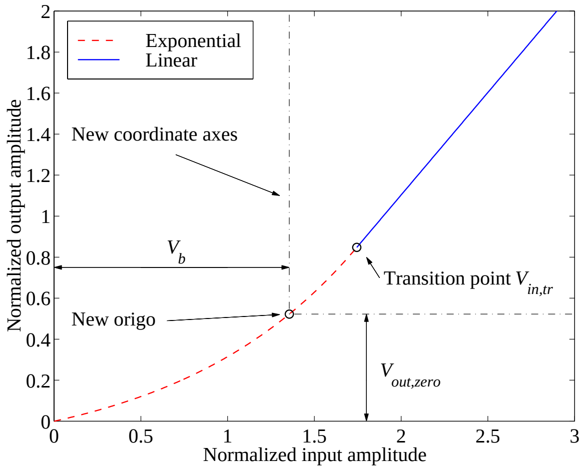

Fig. 1: Impact of the bias parameter V_b on the amplitude distortion curve.

Furthermore, the two-tone test analysis of the HPA revealed that there is a distortion phenomenon at very low power levels separate from the exponential nature. This distortion cannot be seen in the gain measurement curves because it is concealed by the noise which overrules the weak wanted signal. It is presumed that this distortion is due to the weak conduction of the transistors at low power levels, and its influence on the output of the device is taken into account in the model with a cross-over factor

$$C(V_{in}) = \left[\tanh(|V_{in}|)\right]^{\frac{1}{c}} \quad (6)$$

where the parameter c controls the speed of C to change from zero to one.

Since it is presumed that the behaviour of the amplifier is identical with both positive and negative voltages, the final output voltage given by the model is

$$V_{out}(V_{in}) = \frac{\mathrm{sgn}(V_{in})\cdot V'_{out}(|V_{in}|)}{\left[1+\left(\frac{V'_{out}(|V_{in}|)}{A_0}\right)^{2p}\right]^{\frac{1}{2p}}}\left[\tanh(|V_{in}|)\right]^{\frac{1}{c}} \quad (7)$$

where A_0 is the limiting output amplitude ($A_0 \ge 0$) and p is the smoothness parameter defining the transition smoothness from the linear region to the saturated region ($p \ge 0$). The amplitude envelope transfer characteristic of an imaginary amplifier are shown in Fig. 2.

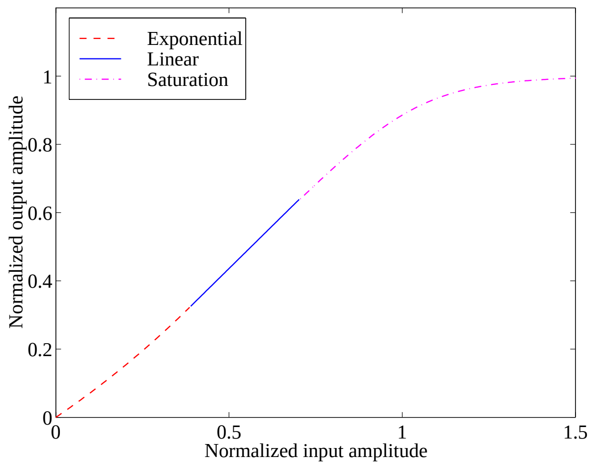

Fig. 2: An example of amplitude envelope transfer characteristics provided by the model.

B. Phase Distortion Model

The phase distortion curve of the modelled HPA has a gently sloping parabolic behaviour in the linear operation region. When the amplifier enters the saturation region the phase change starts to grow quite rapidly. Based on the phase distortion measurements of the HPA, the following function defined piece-wisely was developed to model the relationship between the input amplitude and the relative phase change:

$$\Delta\phi = -r\left(\left|V_{in}\right| - m\right)^2 + \ln\left(1 + e^{s\left(\left|V_{in}\right| - n\right)}\right) \qquad \left|V_{in}\right| < n \tag{8}$$

$$\Delta\phi = 2r(m-n)\left|V_{in}\right| + r\left(n^2 - m^2\right) + \ln\left(1 + e^{s\left(\left|V_{in}\right| - n\right)}\right) \qquad \left|V_{in}\right| \geq n \tag{9}$$

The change from the first part to the second one is continuous because both equations contain the same logarithmic term and the rest of them represents a parabola which changes to a line at $|V_{in}| = n$, where the line has a slope equal to the derivative of the parabola. It should be emphasised that there is no physical basis for the phase distortion function but the function just appears to model the behaviour quite accurately. The parameter r determines the slope of the parabola, and m adjusts the location of the parabola peak. The parameter n adjusts the location of the notch before the phase shift starts to grow, and s controls the slope of the rapidly growing part.

C. Determination of Parameter Values

Parameter values of the amplitude distortion model are determined with multidimensional nonlinear optimisation based on the golden section method [7]. Optimisation minimises the difference between the measured and modelled gain curve. Optimisation interval in case of the amplitude distortion model might be limited to a certain range of the curve in order to obtain a better match in the region of interest. The effect of gain increase due to noise in the low power region and the shape of saturation different from that proposed by the model might lead to an unsatisfactory fit. Due to the minor significance of the phase distortion, parameters of the phase distortion model are evaluated intuitively. Gain and phase shift curves provided by the model are compared to measured curves in Fig. 3.

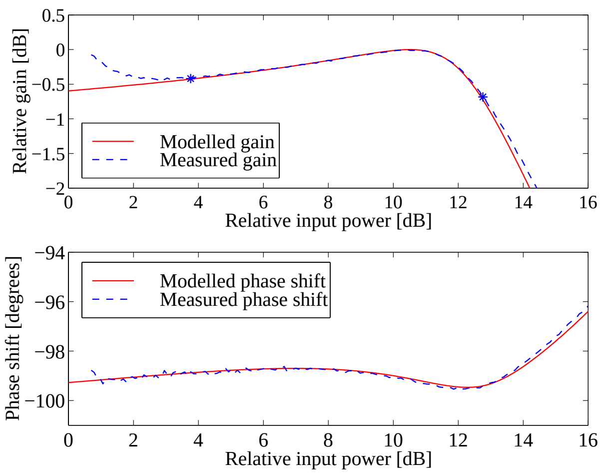

Fig. 3: Modelled and measured gain and phase shift curves. The optimisation interval is indicated by '*' markers.

III. HPA MEASUREMENTS

Since parameter optimisation of the HPA model involves gain and phase shift curves of the modelled HPA, those of a GaAs heterojunction bipolar transistor (HBT) mobile phone amplifier biased to Class AB operation were measured. A two-tone test with 20 dB power sweep and tone frequencies of 835.9 MHz and 836.1 MHz was also carried out because of its generality in nonlinearity characterisation of HPAs. The spectrum regeneration measurements were performed with a π/4-DQPSK signal fulfilling IS-54 specifications [8]. An input power sweep of 21 dB with 1 dB step was made to study the spectral spreading, and the output spectrum of the HPA at each input power level was stored with frequency resolution of 525 Hz for further analysis. The spectral regrowth measurement setup is shown in Fig. 4.

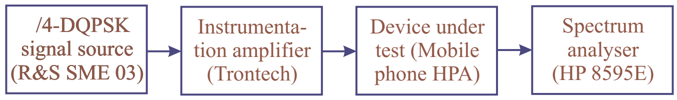

Fig. 4: Spectrum regeneration measurement configuration of π/4-DQPSK modulated IS-54 signal.

IV. TWO-TONE TEST VERIFICATION

Applicability of the model is first evaluated with a two-tone test simulation. Power-swept two-tone signal is applied to the HPA model, and intermodulation distortion (IMD) product powers in the output are found out by taking an FFT from the distorted signal at each power level.

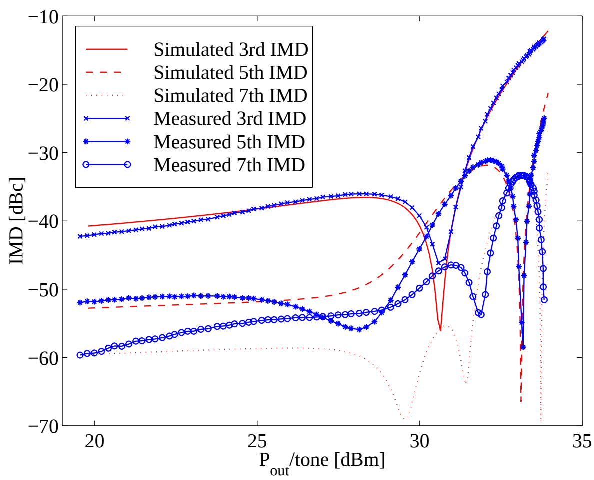

Fig. 5: Simulated and measured intermodulation products in a two-tone test.

Simulated and measured IMD products are compared in Fig. 5. The third-order product is very accurately modelled, and even the notch close to the saturation is correctly produced. The fifth-order product also follows the measured curve closely, except at the shallow notch before the saturation region where the model overstates the IMD product. Clearly, the model is not capable of copying the seventh-order product behaviour as well as those of the lower-orders. Altogether, the agreement between modelled and measured intermodulation behaviour is good.

V. SIMULATION OF SPECTRUM REGENERATION

The configuration of the spectral regrowth simulation with lowpass equivalent signals is shown in Fig. 6. The signal comprises pseudorandom π/4-DQPSK symbols sampled 20 times the symbol rate to make the significant intermodulation products visible in the spectrum. The pulse shape filtering is performed with a time domain realisation of a root-raised cosine filter the parameters of which are determined by the IS-54 standard [8]. The filter is further adjusted to produce a signal whose spectral purity equals that of the measured spectrum from the signal generator. The power of the filtered signal is scaled appropriately to generate a power sweep with 1 dB step, and the signal is amplified with an amplifier model representing the minor nonlinearity of the instrumentation amplifier. Lowpass models of HPA phase and amplitude distortion introduce the nonlinearity of the mobile phone HPA. Additive white Gaussian noise is added to the signal to bring in the effect of a noise floor. Last, the power spectral density is computed with the Bartlett window and it is averaged over 128 2048-point FFT frames.

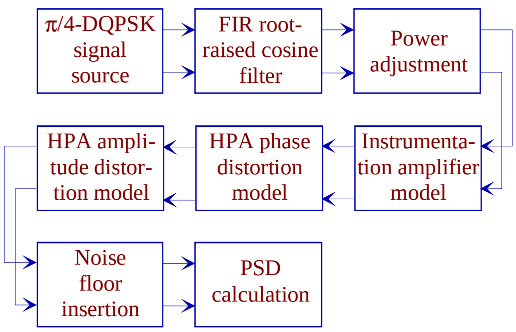

Fig. 6: Block diagram for spectrum regeneration simulation.

VI. COMPARISON BETWEEN SIMULATED AND MEASURED π/4-DQPSK ADJACENT CHANNEL POWER

Those power sweep levels where the spectrum regeneration really starts to raise adjacent channel interference from the inherent minimum levels are of special significance. Illustrations of the good agreement between measured and simulated spectra of nonlinearly amplified π/4-DQPSK signal at two relative input power levels of interest are given in Fig. 7 and Fig. 8.

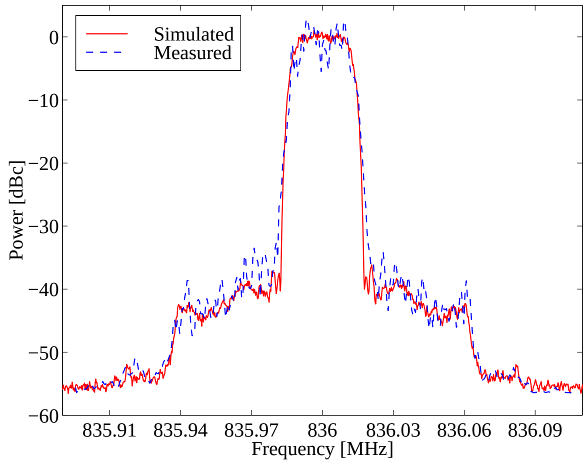

Fig. 7: Measured and simulated spectrum of a nonlinearly amplified π/4-DQPSK signal at the relative input power level 13 dB.

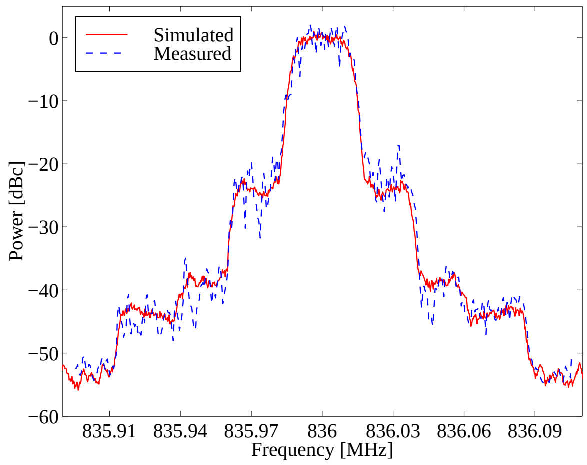

Fig. 8: Measured and simulated spectrum of a nonlinearly amplified π/4-DQPSK signal at the relative input power level 16 dB.

A set of these spectra obtained from the power sweep were filtered with an ideal IS-54 channel filter to extract the spectral skirt power falling on the adjacent channels. The channel filter frequency responses of the first three adjacent channels with a roll-off parameter value $\alpha = 0.35$ are illustrated in Fig. 9. The adjacent channel power ratio (ACPR) is defined as

$$ACPR = \frac{\int_{-\infty}^{\infty} \left| H_{RRC}(f + n\Delta f) \right|^2 S(f)\,df}{\int_{-\infty}^{\infty} \left| H_{RRC}(f) \right|^2 S(f)\,df} \qquad (10)$$

where $S(f)$ is the measured or simulated power spectral density, $H_{RRC}(f)$ represents the root-raised cosine filter, Δf is the channel separation, and n determines the adjacent channel in question. ACPR is averaged over the two channels on both sides of the desired channel, and it is plotted in Fig. 10 for the first three adjacent channels.

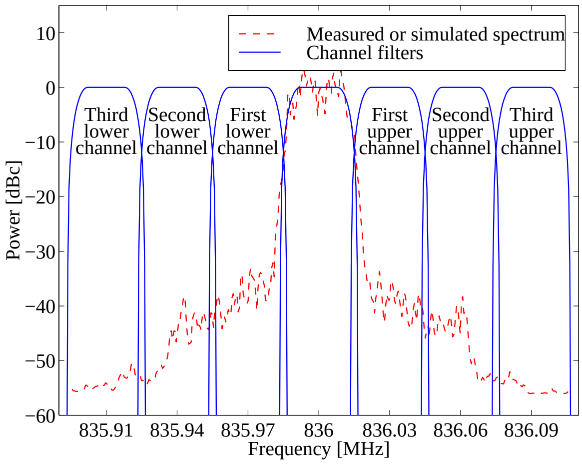

Fig. 9: Channel filtering in the determination of adjacent channel power ratios.

An excellent agreement between measured and simulated ACPR is observed in Fig. 10, especially in case of the first adjacent channel where the error is less than 1.5 dB except in one measurement point. It must be noted that the measured data is not averaged over multiple frequency sweeps as is the case for simulated results where multiple FFT blocks were used to determine the power spectral density. Hence, certain deviation around the expected ACPR level might exist, and that should be considered when comparing the results. The second and third ACPR curves experience a descending slope at low power levels due to the limitations in the dynamic range of the measurement, but at the region of interest they also have a good match, for the difference exceeds 3 dB at only one input power level in deep saturation. Moreover, similar ACPR comparisons made in multiple bias conditions different from the one presented here also yielded very satisfactory agreements.

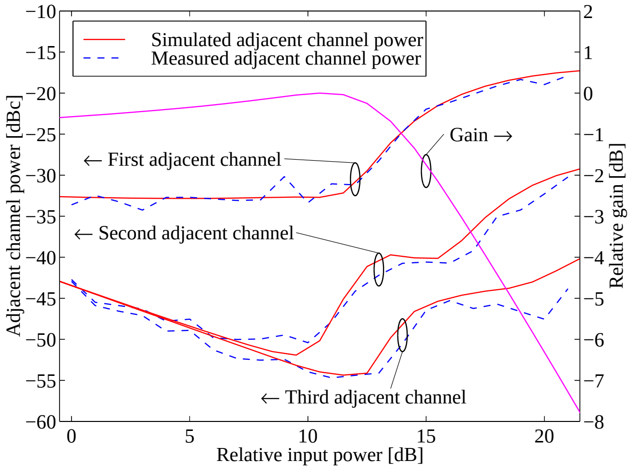

Fig. 10: Measured and simulated adjacent channel power ratios for an IS-54 signal as a function of the relative input power.

VII. CONCLUSIONS

Spectrum regeneration and two-tone test properties of the functional bipolar HPA model [5] featuring an adjustable exponential behaviour on the linear range of the amplitude transfer characteristic are studied by means of simulation. An excellent agreement between measured and simulated adjacent channel powers is found, particularly in case of the first adjacent channel. This together with a good match between measured and simulated two-tone test results suggest that the model copies bipolar high power amplifier characteristics accurately, and thus it is a clear improvement in HPA modelling in radio communication system simulation.

ACKNOWLEDGEMENTS

The work was financed by Technology Development Center of Finland, Nokia, Telecom Finland and Helsinki Telephone Company. The support of Kordelin Foundation to Mr. Honkanen is gratefully acknowledged.

REFERENCES

[1] T. Ojanperä, J. Sköld, J. Castro, L. Girard, and A. Klein, “Comparison of Multiple Access Schemes for UMTS”, *Proc. IEEE 47th Vehicular Tech. Conf. VTC ’97*, Phoenix, USA, May 4-7 1997, pp. 490-494.

[2] J. F. Sevic, and J. Staudinger, ”Simulation of Power Amplifier Adjacent-Channel Power Ratio for Digital Wireless Communication Systems”, *Proc. IEEE 47th Vehicular Tech. Conf. VTC ’97*, Phoenix, USA, May 4-7 1997, pp. 681-685.

[3] S. Ariyavisitakul, and T.-P. Liu, “Characterizing the Effects of Nonlinear Amplifiers on Linear Modulation for Digital Portable Radio Communications”, *IEEE Trans. Vehicular Tech.*, Vol. 39, No. 4, Nov. 1990, pp. 383-389.

[4] S.-W. Chen, W. Panton, and R. Gilmore, “Effects of Nonlinear Distortion on CDMA Communication Systems”, *IEEE Trans. Microwave Theory and Techniques*, Vol. 44, No. 12, December 1996, pp. 2743-2750.

[5] M. Honkanen, and S.-G. Häggman, “New Aspects on Nonlinear Power Amplifier Modeling in Radio Communication System Simulations”, *Proc. IEEE Int. Symp. on Personal, Indoor, and Mobile Radio Comm. PIMRC ’97*, Helsinki, Finland, September 1-4, 1997, pp. 844-848.

[6] C. Rapp, “Effects of HPA-Nonlinearity on a 4-DPSK/OFDM-Signal for a Digital Sound Broadcasting System“, *Proc. 2nd European Conf. on Satellite Communications*, Liege, Belgium, October 22-24, 1991, pp. 179-184.

[7] M. S. Bazaraa, H. D. Sherali and C. M. Betty, *Nonlinear Programming, Theory and Algorithms*, New York: Wiley, 1993, pp. 270-272.

[8] TIA/EIA IS-54, “Cellular System Dual-Mode Mobile Station-Base Station Compatibility Standard”, Telecommunications Industry Association, 1992.